Inorganic Chemistry

ARTICLE

pubs.acs.org/IC

Germanium Selenophosphates: The Incommensurately Modulated $^1/_\infty[Ge_{4-x}P_xSe_{12}^{4-}]$ and the Molecular $[Ge_2P_2Se_{14}]^{6-}$

Collin D. Morris, Christos D. Malliakas, and Mercouri G. Kanatzidis*

Department of Chemistry, Northwestern University, Evanston, Illinois 60208, United States

Supporting Information

ABSTRACT: The new germanium selenophosphates $K_4Ge_{4-x}P_xSe_{12}$ (**1**) and $Rb_6Ge_2P_2Se_{14}$ (**2**) are reported. The former is a one-dimensional metastable compound synthesized using the polychalcogenide flux method that crystallizes in the monoclinic space group $P2_1/c$ with lattice parameters a = 6.7388(7) Å, b = 13.489(1) Å, c = 6.3904(6) Å, and β = 91.025(8)°. At a glance, a mixed Ge^{4+}/P^{5+} tetrahedral site and disordered Se position are found among the corner sharing tetrahedra that make up the polymeric anion. After careful examination, the structure was found to be incommensurately modulated and a single q-vector of q = 0.4442(6)a* + 0.3407(6)c* was determined after annealing single crystals below their decomposition point for 30d. The latter compound contains the new discrete molecular anion $[Ge_2P_2Se_{14}]^{6-}$ and crystallizes in $P\bar{1}$ with lattice parameters a = 7.2463(8) Å, b = 9.707(1)Å, c = 11.987(1)Å, α = 79.516(9)°, β = 89.524(9)°, and γ = 68.281(9)°. Both compounds are semiconductors with band gaps of **1** and **2** being 1.9 eV and 2.2 eV, respectively.

INTRODUCTION

Synthesis of novel alkali metal chalcophosphates has been successful in part because of the polychalcogenide flux method, which allows metastable phases to be accessed at relatively low temperatures (200−600 °C).[1−3] The resulting structures often contain new complex anions that vary in dimensionality and are built of simpler species such as tetrahedral $[PQ_4]^{3-}$ and ethane-like $[P_2Q_6]^{4-}$ moieties (Q = S, Se). Examples of these anions include $[P_8Se_{18}]^{6-}$,[4] $[P_5Se_{12}]^{5-}$,[5] α- and β-$[P_6Se_{12}]^{4-}$,[5,6] $^1/_\infty[PSe_6^-]$,[7] $^1/_\infty[P_2Se_6^{2-}]$,[8] $[P_2S_{10}]^{4-}$,[9] and $[P_2S_8]^{4-}$.[10] Addition of a second main group element to the reaction mixture can result in even more complex structures by further linking the chalcophosphate anions.[11−15] Recently, we reported on the stability of arsenic containing chalcophosphates, some of which feature novel structures.[16] In this paper, we explore the addition of germanium to a selenophosphate flux. Chalcogermanates display a wide structural diversity similar to the chalcophosphates with building moieties such as $[GeQ_4]^{4-}$,[17,18] $[Ge_2Q_6]^{4-}$,[19−21] $[Ge_2Q_6]^{6-}$,[22−25] $[Ge_2Q_8]^{4-}$,[26,27] $[Ge_4Q_{10}]^{4-}$,[28,29] $^1/_\infty[GeSe_3^{2-}]$,[30] and $^1/_\infty[GeSe_4^{2-}]$.[31] Chalcophosphates and chalcogermanates both have technological relevance in areas such as nonlinear optics[5,8,32−34] and ferroelectrics,[35−37] with the chalcogermanates also being used in the synthesis of porous chalcogels[38,39] and zeolite-like anionic frameworks.[40] Herein, we discuss the synthesis of the first reported germanium chalcophosphates. $K_4Ge_{4-x}P_xSe_{12}$ (**1**) is a metastable compound that forms only with a very specific flux composition. Its one-dimensional polymeric structure presents a unique example of an incommensurately modulated motif and contains mixed Ge and P sites as well as Se^{2-} and Se_2^{2-} units. $Rb_6Ge_2P_2Se_{14}$ (**2**) is a discrete molecular salt compound with a new molecular germanium selenophosphate anion.

EXPERIMENTAL SECTION

Reagents. All reagents were used as obtained: potassium metal (98%, Sigma Aldrich, St. Louis, MO); Ge powder (99.999%, Alfa Aesar, Ward Hill, MA); red phosphorus powder (99%, Sigma Aldrich, St. Louis, MO); selenium pellets (99.99%, Sigma Aldrich, St. Louis, MO); *N*,*N*′-dimethylformamide (ACS grade, Mallinckrodt Chemical, Phillipsburg, NJ); diethyl ether (ACS grade, BDH Chemicals, Leicestershire, UK). K_2Se was prepared by reacting stoichiometric amounts of the elements in liquid ammonia as described elsewhere.[41,42] P_2Se_5 was synthesized by the stoichiometric reaction of red P and Se at 460 °C for 48 h followed by cooling to room temperature in 10 h.

Synthesis. Red crystals of $K_4Ge_{4-x}P_xSe_{12}$ were synthesized by the reaction of K_2Se, Ge, P_2Se_5, and Se in a 2:2:1:7 mmol ratio. In a typical reaction, 0.063 g (0.40 mmol) of K_2Se, 0.029 g (0.40 mmol) of Ge, 0.093 g (0.20 mmol) of P_2Se_5 and 0.111 g (1.40 mmol) of Se were added to a 9 mm fused silica tube inside a N_2-filled glovebox. The tube was flame-sealed under a vacuum of $<10^{-4}$ mbar and placed in a temperature controlled furnace. The highest quality crystals resulted by heating to 400 °C in 4 h, dwelling there for 3 h, cooling to 300 °C over 3 h, dwelling there for 3 h, heating to 350 °C over 3 h, dwelling there for 3 h, cooling to 200 °C over 3 h, and then turning off the furnace. The products were washed with degassed dimethylformamide (DMF) for 3 days and dried with diethyl ether to reveal red rod crystals in ∼10% yield (based on potassium). Although the yields of these reactions are very low, pure products resulted when the large excess of flux was dissolved by DMF. Annealed crystals were required for determining the modulated structure of **1**. Isolated single crystals were sealed under vacuum in a fused silica tube, heated to 350 °C over 4 h, held there for 30 days, and cooled to 200 °C over 30 h and to room temperature in 3 h.

Yellow crystals of $Rb_6Ge_2P_2Se_{14}$ were first obtained while trying to synthesize the Rb analog of $K_4Ge_{4-x}P_xSe_{12}$. Once the composition was determined from the structure solution, stoichiometric reaction of 0.150 g (0.60 mmol) of Rb_2Se, 0.029 g (0.40 mmol) of Ge, 0.091 g (0.20 mmol) of P_2Se_5, and 0.095 g (1.20 mmol) of Se in a 9 mm fused silica tube sealed under vacuum (10^{-4} mbar) at 500 °C for 3 days followed by cooling to 200 °C over 60 h and then to room temperature over 3 h led

Received: June 10, 2011
Published: September 19, 2011

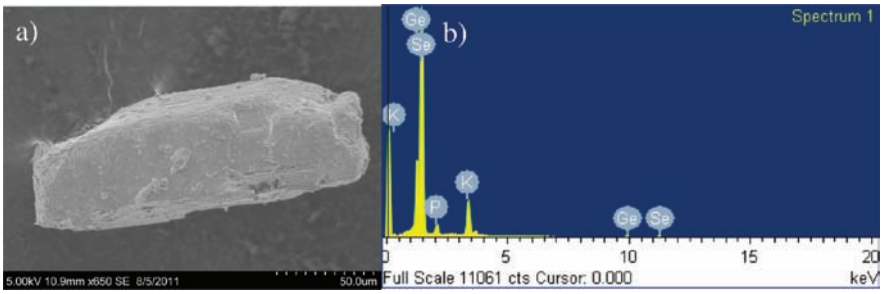

Figure 1. (a) SEM micrograph of typical $K_4Ge_{4-x}P_xSe_{12}$ crystal and (b) corresponding EDS spectrum. EDS consistently confirmed the presence of phosphorus with an average overall composition of $K_{2.4}Ge_{1.6}P_{1.0}Se_{7.5}$.

Table 1. Crystallographic Refinement Details for Reported Compounds

compound	1	2
Formula	$K_4Ge_{2.5}P_{1.5}Se_{12}$	$Rb_6Ge_2P_2Se_{14}$
Formula Weight	1311.04	1825.38
Temperature, K	100	293
Crystal system	Monoclinic	Triclinic
Space group	$P2_1/c$	$P\bar{1}$
a, Å	6.7388(7)	7.2463(8)
b, Å	13.4894(12)	9.7071(11)
c, Å	6.3904(6)	11.9866(14)
α, °	90.00	79.516(9)
β, °	91.025(8)	89.524(9)
γ, °	90.00	68.281(9)
V, Å^3	580.81(10)	768.60(15)
Z	1	1
ρ, mg/m^3	3.748	3.944
μ, mm^{-1}	22.228	28.066
$F(000)$	578	792
θ_{max}, °	29.16	29.24
Reflections collected	5044	14609
Unique reflections	1555	4135
R_{int}	0.0455	0.0432
No. parameters	57	109
Refinement method	full-matrix least-squares on F^2	
GooF	1.240	1.295
Final R indices [$I > 2\sigma(I)$], R_1/wR_2	0.0395/0.0747	0.0454/0.0755
R indices (all data), R_1/wR_2	0.0439/0.0760	0.0597/0.0785

$R_1 = \Sigma||F_o| - |F_c||/\Sigma|F_o|$. $wR_2 = \{\Sigma[w(|F_o|^2 - |F_c|^2)^2]/\Sigma[w(|F_o|^4)]\}^{1/2}$ and calc $w = 1/[\sigma^2(F_o^2) + (0.0176P)^2 + 3.9986P]$ where $P = (F_o^2+2F_c^2)/3$.

to **2** as the major phase. $Rb_6Ge_2P_2Se_{14}$ could not be obtained as a pure phase; however, washing the products with degassed DMF for 1 day followed by rinsing with diethyl ether revealed yellow crystals of **2** in ~80% yield.

Single Crystal X-ray Diffraction. Single crystal X-ray diffraction data were collected by performing ω scans on a STOE IPDS II diffractometer using Mo Kα radiation (λ = 0.71073 Å) operating at 50 kV and 40 mA. Collection, integration, and numerical absorption corrections were performed using the X-AREA, X-RED, and X-SHAPE programs.[43] Structures were solved using direct methods and refined by full-matrix least-squares on F^2 using the SHELXTL program package.[44] For the determination of the modulated structure, diffraction data for the annealed crystals were collected with an increased X-ray exposure time in order to enhance the intensity of the satellite reflections.

Table 2. Atomic Coordinates, Occupancies, and Equivalent Isotropic Displacement Parameters (Å^2) for the Subcell of $K_4Ge_{4-x}P_xSe_{12}$

Label	x	y	z	Occupancy	U_{eq}[a]
Se(1)	0.06970(8)	0.30337(4)	0.30496(7)	1	0.02579(11)
Se(2)	0.24244(6)	0.03214(3)	0.22789(6)	1	0.01652(9)
Se(3A)	0.55995(14)	0.26286(8)	0.14270(18)	0.4341(13)	0.0177(2)
Se(3B)	0.56607(11)	0.24888(6)	0.03283(15)	0.5659(13)	0.01843(19)
Ge(1)	0.24808(8)	0.18698(4)	0.11823(8)	0.634(3)	0.01268(14)
P(1)	0.24808(8)	0.18698(4)	0.11823(8)	0.366(3)	0.01268(14)
K(1)	0.26015(14)	0.53807(8)	0.22533(14)	1	0.01924(19)

[a] U_{eq} is defined as one-third of the trace of the orthogonalized U_{ij} tensor.

The distortion (positional or temperature parameter) of a given atomic parameter x_4 in the subcell can be expressed by a periodic modulation function $p(x_4)$ in a form of a Fourier expansion:

$$p(k + x_4) = \sum_{n=1}^{m} A_{sn} \sin[2\pi\bar{q}_n(k + x_4)] + \sum_{n=1}^{m} A_{cn} \cos[2\pi\bar{q}_n(k + x_4)]$$

where A_{sn} is the sinusoidal coefficient of the given Fourier term, A_{cn} is the cosine coefficient, n is the number of modulation waves used for the refinement, and k is the lattice translation. $\bar{q}_n = \Sigma_{i=1}^{d} \alpha_{ni} q_i$ where α_{ni} is the integer number for the linear combination of the incommensurate modulation vectors q_i. A useful coordinate t that characterizes and describes the real three-dimensional structure constructed as a perpendicular intersection with the fourth dimensional axis is defined as $t = x_4 - \mathbf{q}\cdot\mathbf{r}$ where $\mathbf{r}$ is a vector in the real three-dimensional reciprocal space. Satellite reflections of first order were observed at 100 K and used for the refinement. One modulation wave for occupantional, positional, and temperature parameters was used. Fourier terms were refined on the basis of the symmetry allowed conditions. Structure refinement of the supercell was performed with Jana2006.[45]

Powder X-ray Diffraction (PXRD). A National Institute of Standards and Technology (NIST) Si calibrated CPS 120 INEL powder X-ray diffractometer (Cu Kα graphite monochromatized radiation) equipped with a position sensitive detector, operating at 40 kV and 20 mA, was used to determine the phase-purity of all products. A flat sample geometry was used for collection. Simulated patterns were created using the Visualizer program in Findit and the CIF of each structure solution.

Scanning Electron Microscopy (SEM). A Hitachi S-3500 scanning electron microscope (SEM) equipped with a PGT energy dispersive

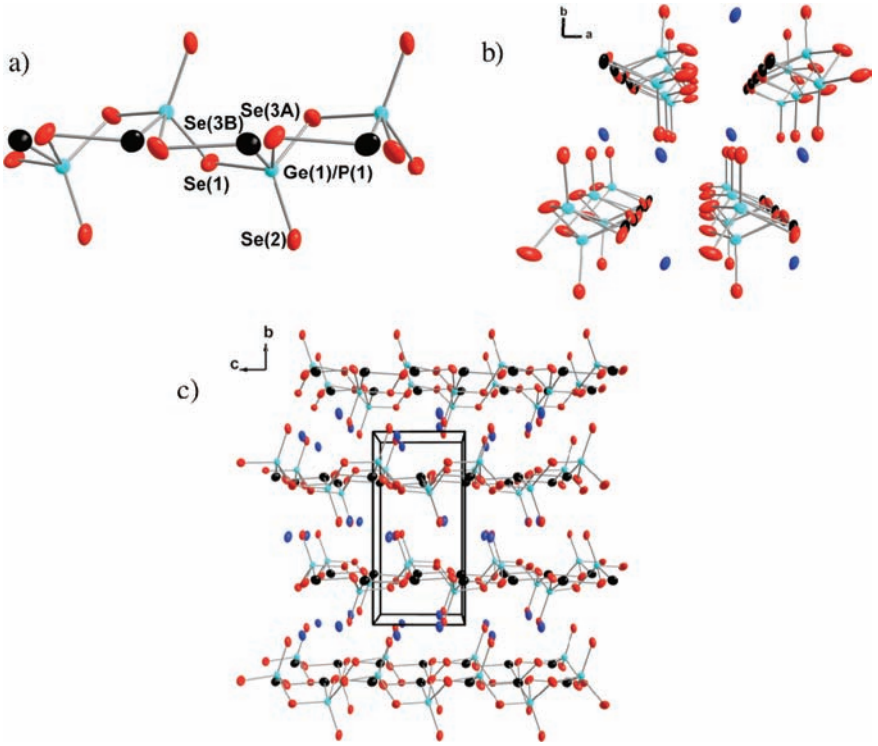

Figure 2. Structure of $K_4Ge_{4-x}P_xSe_{12}$ with thermal ellipsoids set to 80%. (a) View of anionic linear chain perpendicular to its direction of propogation. (b) Packing of chains as viewed down the *c*-axis. (c) Pseudolayers formed in the *a*,*c*-plane by the stacking of chains directly on top of one another. Color code: K, dark blue; Ge/P, light blue; Se(3A), red; Se(3B), black.

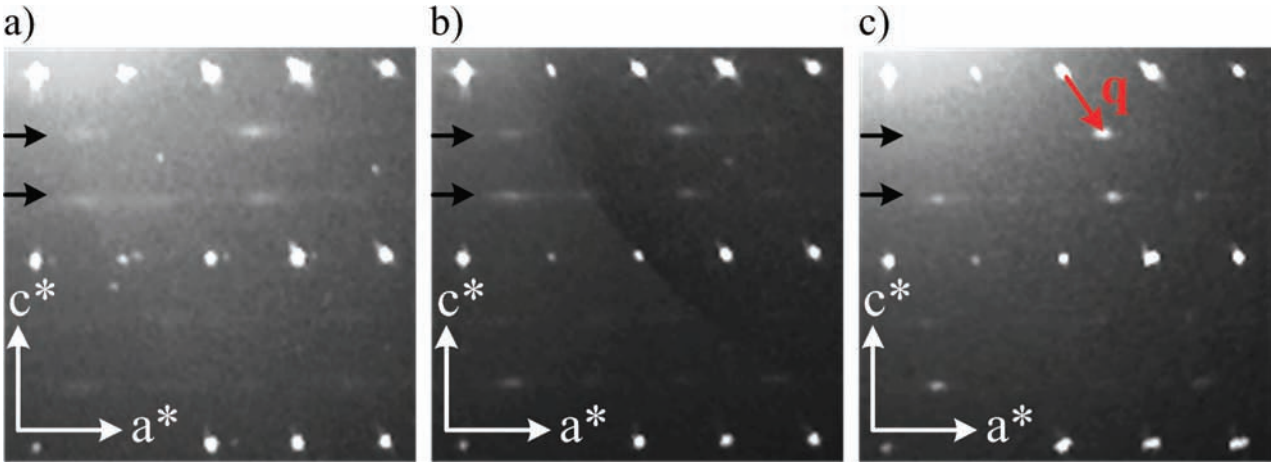

Figure 3. Synthetic precession photographs of $K_4Ge_{4-x}P_xSe_{12}$ viewing the (h 0 l) plane for (a) no annealing, (b) 15 days of annealing, and (c) 30 days of annealing samples. The direction of diffuse intensity is shown with arrows on each figure. Diffuse reflections at $\sim(^1/_2\ 0\ ^1/_3)$ became sharper upon annealing and were then indexed and used to determine the superstructure of **1**. The modulation q-vector is also indicated with a red arrow.

X-ray analyzer was used for energy dispersive X-ray spectroscopy (EDS) analysis of crystalline products. An accelerating voltage of 25 kV, probe current of 60 mA, and a 60 s acquisition time were used for data collection.

Solid State UV−Vis Spectroscopy. The band gap of each material was determined by collecting optical diffuse reflectance data on a Shimadzu UV-3101 PC double-beam, double-monochromator spectrophotometer in the range of 200−2500 nm. $BaSO_4$ was used as a 100% reflectance standard and as a bed onto which the ground crystalline sample was packed. The band gap was then estimated by converting the reflectance data to absorbance using the Kubelka−Munk equation: $\alpha/S = (1 - R)^2/(2R)$, where R is the reflectance and α and S are the absorption and scattering coefficients, respectively.[46−48]

Differential Thermal Analysis (DTA). Ground crystalline samples (~40 mg) of each product were sealed under vacuum ($\sim 10^{-4}$ mbar) in a fused silica ampule for differential thermal analysis experiments. A similar amount of Al_2O_3 was used as a reference in a second evacuated ampule. Experiments were performed in a Shimadzu DTA-50 thermal analyzer with a heating and cooling rate of 5 °C/min for each run and a nitrogen flow rate of 40 mL/min.

Raman Spectroscopy. Raman spectra were collected on a Delta-Nu Advantage 785 NIR Spectrometer equipped with a CCD detector.

dx.doi.org/10.1021/ic201249w |*Inorg. Chem.* 2011, 50, 10241–10248

Table 3. Crystal Data and Modulated Structure Refinement Details for 1

Empirical formula	K4 Ge2.731 P1.269 Se12
Formula weight	1341.5
Temperature	100 K
Wavelength	0.71073 Å
Crystal system	monoclinic
Space group	$P2_1(\alpha 0\gamma)0$
Unit cell dimensions	a = 6.7285(6) Å, α = 90°
	b = 13.5089(11) Å, β = 90.875(7)°
	c = 6.3781(6) Å, γ = 90°
q-vector(1)	$0.4442(6)a^* + 0.3407(6)c^*$
Volume	579.67(9) Å^3
Z	1
Density (calculated)	3.8416 g/cm^3
Absorption coefficient	23.152 mm^{-1}
$F(000)$	590
Crystal size	0.15 × 0.10 × 0.05 mm^3
θ range for data collection	1.74 to 29.27°
Index ranges	$-9 \le h \le 9$, $-18 \le k \le 18$, $-9 \le l \le 7$, $-1 \le m \le 1$
Reflections collected	22085 (8009 main +14076 satellites)
Independent reflections	9259 (3107 main +6152 satellites) [R_{int} = 0.0702]
Completeness to θ = 29.27°	98%
Refinement method	Full-matrix least-squares on F^2
Data/constrains/restraints/parameters	9259/23/0/240
Goodness-of-fit on F^2	1.90
Final R indices [$I > 3\sigma(I)$]	R_{obs} = 0.0821, wR_{obs} = 0.1640
R indices [all data]	R_{all} = 0.1736, wR_{all} = 0.2020
Final R main indices [$I > 3\sigma(I)$]	R_{obs} = 0.0605, wR_{obs} = 0.1451
R main indices (all data)	R_{all} = 0.0814, wR_{all} = 0.1594
Final R 1st order satellites [$I > 3\sigma(I)$]	R_{obs} = 0.1762, wR_{obs} = 0.2914
R 1st order satellites (all data)	R_{all} = 0.3586, wR_{all} = 0.4183
T_{min} and T_{max} coefficients	0.0816 and 0.5464
Largest diff. peak and hole	7.00 and −6.00 e·Å^{-3}

$R = \Sigma||F_o| - |F_c||/\Sigma|F_o|$, $wR = \{\Sigma[w(|F_o|^2 - |F_c|^2)^2]/\Sigma[w(|F_o|^4)]\}^{1/2}$ and $w = 1/(\sigma^2(I) + 0.0016I^2)$.

The 785 nm radiation had a maximum power of 60 mW and beam diameter of 35 μm. A collection time of 5 s was used.

RESULTS AND DISUCUSSION

Red crystals of $K_4Ge_{4-x}P_xSe_{12}$ (**1**) were obtained from the reaction of K_2Se, Ge, P_2Se_5, and Se in a 2:2:1:7 molar ratio. The phase can also be synthesized using elemental phosphorus rather than P_2Se_5. The single crystal structure was initially solved in $P2_1/c$ as $K_2Ge_2Se_6$, an analog of the previously reported $Cs_2Si_2Te_6$, containing a disordered Se position.[49] However, upon further investigation, it was determined that this model was incorrect. Phosphorus was consistently present in every crystal we examined by energy dispersive X-ray spectroscopy (EDS) with an average composition of $K_{2.4}Ge_{1.6}P_{1.0}Se_{7.5}$ (Figure 1). Also, several attempts to synthesize the compound without phosphorus as a reactant failed to give the desired product. The refinement was modified to mix the only Ge site with P, and an improvement in all statistics, including a refined Ge/P ratio similar to that observed by EDS (63:37 in refinement, 62:38 in EDS), resulted (Tables 1 and 2). The precise flux composition for this reaction was crucial in producing the desired phase. Attempts to synthesize **1** by direct combination with the structurally refined elemental ratios were unsuccessful, as were reactions aimed to increase the relative amount of phosphorus in the compound. In both cases, the known compounds $K_2P_2Se_6$[50] and Ge_4Se_9[51] were found as products. While attempting to synthesize the Rb analog of **1**, the new compound $Rb_6Ge_2P_2Se_{14}$ (**2**) was discovered. Several attempts to obtain **2** as a pure phase were unsuccessful and always showed the presence of an unknown impurity by powder X-ray diffraction and differential thermal analysis.

Structure of $K_4Ge_{4-x}P_xSe_{12}$. The basic structural motif of **1** consists of an infinite linear chain of corner sharing MSe_4 (M = Ge, P) tetrahedra that form a diselenide bond with one neighboring tetradedron to give a five-membered M_2Se_5 ring (Figure 2). The chains propagate along the c-axis and stack directly on top of one another along the a-axis to form a pseudolayered structure in the a,c-plane. $K_4Ge_{4-x}P_xSe_{12}$ can be described as a variant of certain previously reported I/III/VI and I/IV/VI compounds with 1:1:3 compositions. ABS_3 (A = Rb, Tl),[52] $ABSe_3$ (A = Rb, Cs),[53] $CsGaQ_3$ (Q = S, Se),[54,55] and $CsAlTe_3$[56] are all isostructural to one another, crystallize in the same space group as **1**, and contain a similar one-dimensional anion. In the case of these I/III/VI compounds, every Group III metal ion is tetrahedrally coordinated to two bridging chalcogenide ions and two dichalcogenide units, resulting in a linear chain of corner sharing tetrahedra running parallel to the c-axis. $TlBSe_3$[53] contains the same anion but crystallizes in the noncentrosymmetric space group Cc. For the I/IV/VI compounds, $Cs_2Si_2Te_6$[49] also crystallizes in the monoclinic space group Cc but contains a slightly different anion in which each Si ion is tetrahedrally coordinated to two bridging Te ions, one ditelluride and one terminal Te ion. The packing of the anions in $K_4Ge_{4-x}P_xSe_{12}$ is the same as the I/III/VI compounds that crystallize in $P2_1/c$; however, the anion is most similar to that found in $Cs_2Si_2Te_6$. Since **1** also has P^{5+} on the Ge^{4+} site, it must necessarily contain even fewer diselenide units than this I/IV/VI compound. Two other compounds have been reported in this family, $Cs_2Sn_2Q_6$ (Q = S, Se),[57,58] but they form layered structures in which one-dimensional chains of edge sharing trigonal bipyramidal Sn ions are further linked by dichalcogenide units, resulting in a two-dimensional structure.

The structure of **1** is more complex than this because of the positionally disordered Se(3) site and the incorporation of the higher valent P^{5+} on the Ge^{4+} site. A more precise description of the molecular formula can be written as $K_4Ge_{4-x}P_x(Se_2^{2-})_{2-(x/2)}(Se^{2-})_{8+x}$, where $x \approx 1.6$ on the basis of the Ge/P ratios obtained from EDS and the structure refinement. The number of diselenide bonds is dictated by the amount of phosphorus present (or vice versa) in order to achieve charge balance. The closest distance between the disordered atoms Se(3A) and Se(3B) is only 0.729 Å with the next shortest distance being 2.498(1) Å. The latter is in the upper range of what can be considered a diselenide bond, with typical values falling between 2.2 and 2.5 Å. The distances between the same disordered atoms in a single chain are 3.214(1) Å and 3.195(1) Å for Se(3A)−Se(3A) and Se(3B)−Se(3B), respectively. These distances are much too

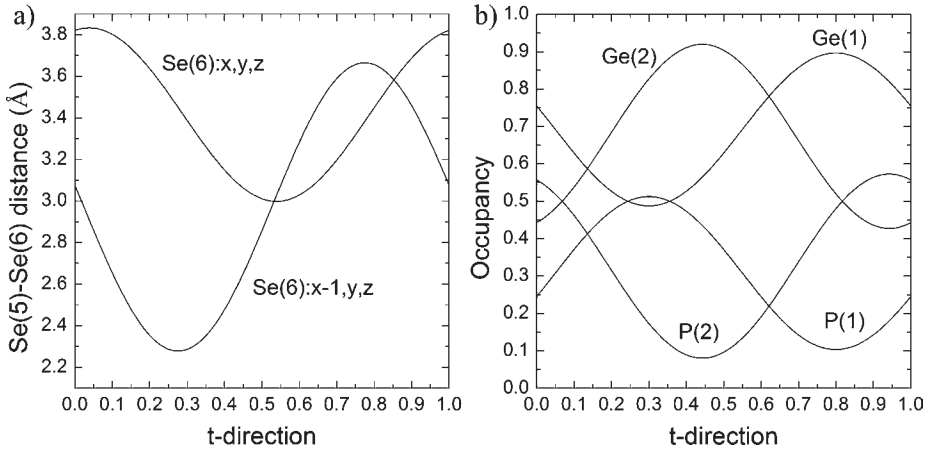

Figure 4. (a) Distribution of Se(5)−Se(6) distances in the supercell model along the modulation direction *t* (see text for details). (b) Occupantional waves for Ge(1), Ge(2), P(1), and P(2) along the modulation direction *t*.

long to be considered a Se−Se bond. All M−Se bond distances are normal and in the range of 2.2037(7)−2.3725(9) Å, with the longest bond distances being between P/Ge and the disordered Se sites (Table S1, Supporting Information).

A closer look at the reciprocal space revealed weak diffuse reflections at roughly ($^1/_2$ *k* $^1/_3$) that were unindexed by the subcell (Figure 3), indicating long-range ordering and structural disorder. In an attempt to reduce the disorder and make the intensity of the supercell reflections more localized, like Bragg reflections, crystals of **1** were annealed at 350 °C for 5, 15, and 30 days. After annealing for 30 days followed by slow cooling (5 °C/h) to 200 °C and to room temperature in 3 h, the extra diffuse reflections had become more localized and were indexed and used to determine the supercell. The structure is therefore incommensurately modulated with a refined single diagonal *q*-vector of $q = 0.4442(6)a^* + 0.3407(6)c^*$ (Figure 3c). A stable refinement was achieved with the monoclinic superspace group $P2_1(\alpha 0\gamma)0$ with an overall agreement factor of 8.2% for the observed reflections (Table 3). The agreement factor for the corresponding distorted subcell was 6.05%, which was greatly improved from the initial value of 30.44% for the subcell without Se disorder.[59] Because of the diffuse nature of the supercell reflections and the elongated thermal motion of the Se(3) atoms, the agreement factor for the observed satellite reflections was 17.6%. The distribution of Se−Se distances of the terminal Se atoms along the infinite chains has an average distance of 2.970(8) Å, a minimum of 2.278(7) Å, and a maximum of 3.665(8) Å. The refined occupancies of Ge and P from the supercell refinement are 1.37(4) and 0.63(4), respectively. Furthermore, a long-range ordering was found for the Ge and P atoms (Figure 4b). The occupantional modulation waves of Ge(1) and P(1) (and Ge(2) and P(2)) were refined as complementary since there is no indication of vacancies on the Ge/P sites. Because of the diagonal orientation of the modulation vector and the presence of occupantional distortion in the Ge/P site, each infinite chain of $K_4Ge_{4-x}P_xSe_{12}$ has a unique distribution of Ge and P atoms along its backbone. Several representative chains are shown in Figure 5.

Structure of $Rb_6Ge_2P_2Se_{14}$. $Rb_6Ge_2P_2Se_{14}$ crystallizes in $P\bar{1}$ and contains a discrete molecular anion made up of a central Ge_2Se_6 moiety capped by a single PSe_4 tetrahedron on each side through a diselenide bond (Table 1, Figure 6). As such, the formula can be expanded and more clearly represented as

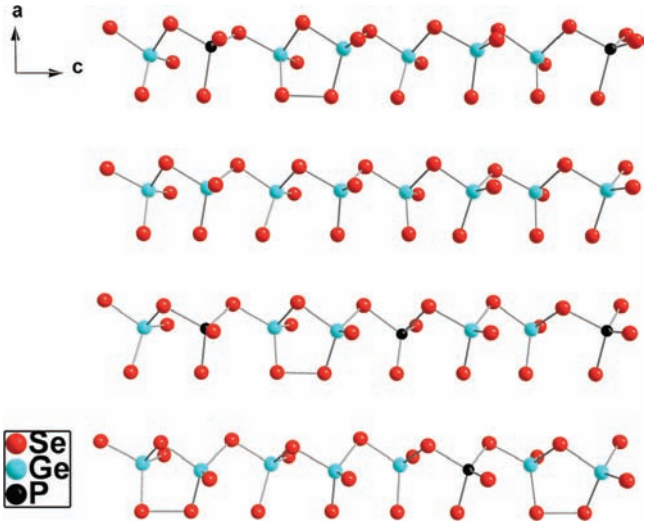

Figure 5. Ball and stick representation of several chains of **1** from the modulated solution as viewed down the *b*-axis. Cutoff for Se−Se bond set at 2.40 Å. Metal sites set as either Ge or P on the basis of occupational waves from Figure 4b using 0.5 as the deciding value.

$Rb_6Ge_2P_2(Se_2^{2-})_2(Se^{2-})_{10}$. Contrary to what is observed in **1**, all main group sites in **2** are element specific and negative occupancies resulted when the sites were mixed (Table S4, Supporting Information). $Rb_6Ge_2P_2Se_{14}$ is an analog of the previously reported compound $A_6Sn_2P_2Se_{14}$ (A = Rb, Cs).[60] Both Group IV selenophosphates have the same packing of their molecular anions, and when comparing their volumes, the cell for the Sn analog is 11% larger than that of **2**. The discrete molecules form a step-like arrangement in the *b*,*c*-plane with nonbonding Se−Se interactions between Se(2) and Se(5) at 3.597(2) Å. They also stack on top of one another to form columns along the *a*-axis with slightly longer Se−Se interactions of 3.686(2) Å between Se(3) and Se(4). This type of packing is reminiscent of that seen in the molecular compounds $K_6P_8Se_{18}$[4] and $K_6As_2(P_2Se_6)_3$,[16] which both showed stepwise packing of columns formed by the stacking of molecular anions. All bond lengths are reasonable with ranges of 2.157(2)−2.287(2) Å for P−Se and 2.2605(9)−2.4100(9) Å for Ge−Se and a Se(4)−Se(5) distance of 2.3360(9) Å (Table S5, Supporting Information).

dx.doi.org/10.1021/ic201249w |*Inorg. Chem.* 2011, 50, 10241–10248

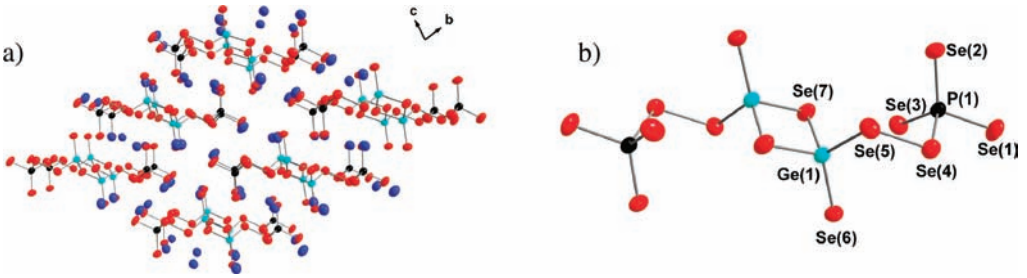

Figure 6. Structure of $Rb_6Ge_2P_2Se_{14}$ showing (a) columnar packing of molecular anions as viewed down the *a*-axis and (b) a single molecular anion of $[Ge_2P_2Se_{14}]^{6-}$. Thermal ellipsoids are set at 80% probability. Color code: Rb, dark blue; Ge, light blue; P, black; Se, red.

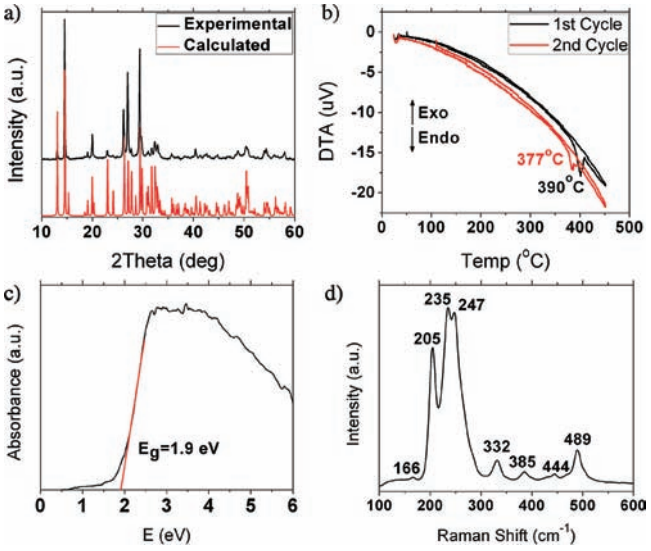

Figure 7. (a) PXRD of **1**. The simulated (red) and experimental (black) patterns are displayed. After washing, the products obtained from the flux reaction are pure. (b) Differential thermal analysis of **1**. Two sequential cycles exhibit slightly different endothermic peaks but no crystallization, implying decomposition. (c) Diffuse reflectance UV−vis spectrum of **1**. A band gap of 1.9 eV matches well with the red color of the crystals. (d) Raman spectrum of **1**. The peak at 239 cm^{-1} can be assigned to the totally symmetric stretch of the MSe_4 (M = Ge, P) tetrahedron and most likely masks the peak for the diselenide stretch. All other peaks can be attributed to various stretches and bends of the molecule.

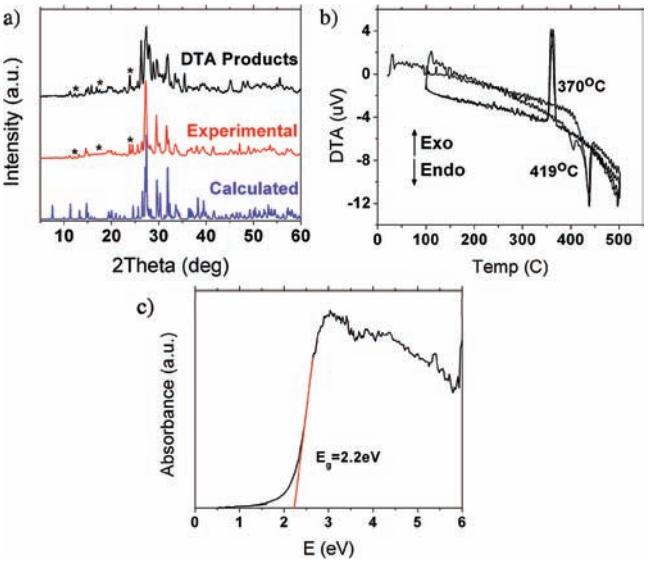

Figure 8. (a) PXRD of **2**. All main peaks match well between the simulated (blue), experimental (red), and post-DTA (black) patterns. Although the major phase **2** melts congruently, indicated by the agreement of the patterns before and after DTA, the impurity peaks (marked by asterisks) are present in both patterns. (b) DTA of **2** showing reproducible melting and crystallization at 419 and 370 °C, respectively. Melting of the minor phase can also be seen at ~400 °C. (c) A band gap of 2.2 eV was estimated from the UV−vis absorption spectrum.

Spectroscopy and Thermal Properties. A band gap of 1.9 eV was estimated from the solid state UV−vis absorption spectrum of $K_4Ge_{4-x}P_xSe_{12}$, which is in agreement with the red color of the crystals (Figure 7). Differential thermal analysis supports the fact that **1** is a metastable phase. A DTA experiment performed on washed products shows a weak endothermic peak at ~390 °C during the first cycle of heating and no exotherm on cooling. A second cycle reveals a slightly shifted endotherm at ~377 °C and again no crystallization. Analysis of the sample by powder X-ray diffraction after two cycles of DTA indicates the partial decomposition of **1** into an unknown phase by the appearance of several new, unmatched peaks. The Raman spectrum of **1** shows numerous peaks between 200 and 500 cm^{-1}. The most intense peaks at 235 cm^{-1} and 247 cm^{-1} arise from the antisymmetric and symmetric stretching modes of the diselenide unit, respectively.[32] The peak at 205 cm^{-1} is attributed to the totally symmetric stretch of the MSe_4 group while the weak peaks below 200 cm^{-1} and above 300 cm^{-1} are due to various bending and stretching modes of the tetrahedral unit, respectively.[32,61]

The presence of a minor phase can be seen in the PXRD (indicated by arrows) and DTA (weak endotherm ~400 °C) of $Rb_6Ge_2P_2Se_{14}$ (Figure 8). Despite the impurity, **2** melts congruently at 419 °C and recrystallizes at 370 °C. All peaks corresponding to the majority phase match well with the simulated pattern before and after DTA as well. The Raman spectrum of **2** has been omitted because of significant interference from the impurity. SEM/EDS analysis of several crystals confirmed the presence of all elements with a composition of $Rb_{6.0}Ge_{2.0}P_{2.2}Se_{12.8}$ (Figure S1, Supporting Information).

CONCLUDING REMARKS

Two new compounds $K_{4-x}Ge_{4-x}P_xSe_{12}$ and $Rb_6Ge_2P_2Se_{14}$ have been synthesized and, to the best of our knowledge, represent the first reported germanium chalcophosphates. Synthesis of **1** as a pure phase was only achieved using the polychalcogenide

flux method and reiterates the importance of this technique in the discovery of new compounds. These compounds with varying dimensionality containing germanium and phosphorus presage a potentially rich family of compounds and can help guide future synthetic efforts. The one-dimensional anion of **1** is complex in that it contains a mixed main group site between Ge and P that orders in the long-range as well as positionally distorted Se atoms that are involved in diselenide bonds. The long-range ordering of the Se atoms and the occupantional distortion of the Ge/P atoms give rise to an incommensurately modulated supercell with a single diagonal q-vector of $q = 0.4442(6)a^* + 0.3407(6)c^*$.

■ ASSOCIATED CONTENT

Supporting Information. SEM micrograph and EDS results of **2**, crystallographic tables, and crystallographic information files (CIFs). This material is available free of charge via the Internet at http://pubs.acs.org.

■ AUTHOR INFORMATION

Corresponding Author
*E-mail: m-kanatzidis@northwestern.edu.

■ ACKNOWLEDGMENT

The SEM/EDS work was performed in the EPIC facility of NUANCE Center at Northwestern University. NUANCE Center is supported by NSF-NSEC, NSF-MRSEC, Keck Foundation, the State of Illinois, and Northwestern University. Financial support from the National Science Foundation (NSF) (DMR-1104965) is gratefully acknowledged.

■ REFERENCES

(1) Kanatzidis, M. G.; Sutorik, A. C. *Prog. Inorg. Chem.* **1995**, *43*, 151.
(2) Kanatzidis, M. G. *Curr. Opin. Solid State Mater. Sci.* **1997**, *2*, 139.
(3) Bensch, W.; Wu, Y. D. *CrystEngComm* **2010**, *12*, 1003.
(4) Chondroudis, K.; Kanatzidis, M. G. *Inorg. Chem.* **1998**, *37*, 2582.
(5) Chung, I.; Jang, J. I.; Gave, M. A.; Weliky, D. P.; Kanatzidis, M. G. *Chem. Commun. (Cambridge, U. K.)* **2007**, 4998.
(6) Chung, I.; Karst, A. L.; Weliky, D. P.; Kanatzidis, M. G. *Inorg. Chem.* **2006**, *45*, 2785.
(7) Chung, I.; Do, J.; Canlas, C. G.; Weliky, D. P.; Kanatzidis, M. G. *Inorg. Chem.* **2004**, *43*, 2762.
(8) Chung, I.; Malliakas, C. D.; Jang, J. I.; Canlas, C. G.; Weliky, D. P.; Kanatzidis, M. G. *J. Am. Chem. Soc.* **2007**, *129*, 14996.
(9) Aitken, J. A.; Canlas, C.; Weliky, D. P.; Kanatzidis, M. G. *Inorg. Chem.* **2001**, *40*, 6496.
(10) Wu, Y. D.; Bensch, W. *Inorg. Chem.* **2007**, *46*, 6170.
(11) Rothenberger, A.; Morris, C.; Wang, H. H.; Chung, D. Y.; Kanatzidis, M. G. *Inorg. Chem.* **2009**, *48*, 9036.
(12) Rothenberger, A.; Morris, C.; Kanatzidis, M. G. *Inorg. Chem.* **2010**, *49*, 5598.
(13) Chung, I.; Song, J. H.; Jang, J. I.; Freeman, A. J.; Ketterson, J. B.; Kanatzidis, M. G. *J. Am. Chem. Soc.* **2009**, *131*, 2647.
(14) Breshears, J. D.; Kanatzidis, M. G. *J. Am. Chem. Soc.* **2000**, *122*, 7839.
(15) Mccarthy, T. J.; Kanatzidis, M. G. *J. Chem. Soc. Chem. Commun.* **1994**, 1089.
(16) Morris, C. D.; Kanatzidis, M. G. *Inorg. Chem.* **2010**, *49*, 9049.
(17) Matsushita, Y.; Kanatzidis, M. G. *Z. Naturforsch., B* **1998**, *53*, 23.
(18) Klepp, K. O. *Z. Naturforsch., B* **1985**, *40*, 878.
(19) Palchilk, O.; Marking, G. M.; Kanatzidis, M. G. *Inorg. Chem.* **2005**, *44*, 4151.
(20) Eisenmann, B.; Hansa, J. *Z. Kristallogr.* **1993**, *203*, 301.
(21) van Almsick, T.; Sheldrick, W. S. *Z. Anorg. Allg. Chem.* **2005**, *631*, 1746.
(22) Eisenmann, B.; Kieselbach, E.; Schafer, H.; Schrod, H. *Z. Anorg. Allg. Chem.* **1984**, *516*, 49.
(23) Marking, G. A.; Kanatzidis, M. G. *J. Alloys Compd.* **1997**, *259*, 122.
(24) Eisenmann, B.; Hansa, J.; Schafer, H. *Mater. Res. Bull.* **1985**, *20*, 1339.
(25) Schlirf, J.; Deiseroth, H. J. *Z. Kristallogr.-New Cryst. Struct.* **2001**, *216*, 27.
(26) Wu, Y. D.; Nather, C.; Bensch, W. *Acta Crystallogr., Sect. E* **2003**, *59*, I137.
(27) Sheldrick, W. S.; Schaaf, B. *Z. Naturforsch., B* **1994**, *49*, 655.
(28) Philippo., E; Ribes, M.; Lindqvis., O *Rev. Chim. Miner.* **1971**, *8*, 477.
(29) Eisenmann, B.; Hansa, J. *Z. Kristallogr.* **1993**, *206*, 101.
(30) Eisenmann, B.; Hansa, J.; Schafer, H. *Z. Naturforsch., B* **1985**, *40*, 450.
(31) Sheldrick, W. S.; Schaaf, B. *Z. Naturforsch., B* **1995**, *50*, 1469.
(32) Chung, I.; Jang, J.-I.; Malliakas, C. D.; Ketterson, J. B.; Kanatzidis, M. G. *J. Am. Chem. Soc.* **2010**, *132*, 384.
(33) Liao, J. H.; Marking, G. M.; Hsu, K. F.; Matsushita, Y.; Ewbank, M. D.; Borwick, R.; Cunningham, P.; Rosker, M. J.; Kanatzidis, M. G. *J. Am. Chem. Soc.* **2003**, *125*, 9484.
(34) Kim, Y.; Seo, I. S.; Martin, S. W.; Baek, J.; Halasyamani, P. S.; Arumugam, N.; Steinfink, H. *Chem. Mater.* **2008**, *20*, 6048.
(35) Carpentier, C. D.; Nitsche, R. *Mater. Res. Bull.* **1974**, *9*, 1097.
(36) Scott, B.; Pressprich, M.; Willet, R. D.; Cleary, D. A. *J. Solid State Chem.* **1992**, *96*, 294.
(37) Tampier, M.; Johrendt, D. *J. Solid State Chem.* **2001**, *158*, 343.
(38) Bag, S.; Trikalitis, P. N.; Chupas, P. J.; Armatas, G. S.; Kanatzidis, M. G. *Science* **2007**, *317*, 490.
(39) Bag, S.; Kanatzidis, M. G. *J. Am. Chem. Soc.* **2008**, *130*, 8366.
(40) Rothenberger, A.; Shafaei-Fallah, M.; Kanatzidis, M. G. *Inorg. Chem.* **2010**, *49*, 9749.
(41) McCarthy, T. J.; Ngeyi, S. P.; Liao, J. H.; DeGroot, D. C.; Hogan, T.; Kannewurf, C. R.; Kanatzidis, M. G. *Chem. Mater.* **1993**, *5*, 331.
(42) (a) Mccarthy, T. J.; Kanatzidis, M. G. *Inorg. Chem.* **1995**, *34*, 1257. (b) Chondroudis, K.; McCarthy, T. J.; Kanatzidis, M. G. *Inorg. Chem.* **1996**, *35*, 840.
(43) Stoe X-Area, Version 1.55; Stoe & Cie GmbH: Darmstadt, Germany, 1998.
(44) Sheldrick, G. M. *Acta Crystallogr., Sect. A* **2008**, *64*, 112.
(45) Petricek, V.; Dusek, M.; Palatinus, L. Jana 2006. Structure Determination Software Programs; Institute of Physics: Praha, Czech Republic, 2006.
(46) Kortüm, G. *Reflectance spectroscopy. Principles, methods, applications*; Springer: Berlin, Heidelberg, New York, 1969.
(47) Chung, D. Y.; Hogan, T.; Schindler, J.; Iordanidis, L.; Brazis, P.; Kannewurf, C. R.; Chen, B.; Uher, C.; Kanatzidis, M. G. *Thermoelectric Mater.-New Dir. Approaches* **1997**, *478*, 333.
(48) Stephan, H. O.; Kanatzidis, M. G. *Inorg. Chem.* **1997**, *36*, 6050.
(49) Brinkmann, C.; Eisenmann, B.; Schafer, H. *Mater. Res. Bull.* **1985**, *20*, 1285.
(50) Kanatzidis, M. G.; Chung, I.; Malliakas, C. D.; Jang, J. I.; Canlas, C. G.; Weliky, D. P. *J. Am. Chem. Soc.* **2007**, *129*, 14996.
(51) Fjellvag, H.; Kongshaug, K. O.; Stolen, S. *J. Chem. Soc. Dalton* **2001**, 1043.
(52) Puttmann, C.; Hiltmann, F.; Hamann, W.; Brendel, C.; Krebs, B. *Z. Anorg. Allg. Chem.* **1993**, *619*, 109.
(53) Lindemann, A.; Kuper, J.; Hamann, W.; Kuchinke, J.; Koster, C.; Krebs, B. *J. Solid State Chem.* **2001**, *157*, 206.
(54) Devi, M. S.; Vidyasagar, K. *J. Chem. Soc. Dalton* **2002**, 4751.
(55) Kanatzidis, M. G.; Do, J. *Z. Anorg. Allg. Chem.* **2003**, *629*, 621.
(56) Eisenmann, B.; Jager, J. *Z. Kristallogr.* **1991**, *197*, 251.
(57) Liao, J. H.; Varotsis, C.; Kanatzidis, M. G. *Inorg. Chem.* **1993**, *32*, 2453.

(58) Loose, A.; Sheldrick, W. S. *Z. Naturforsch., B* **1998**, *53*, 349.
(59) Table 1 presents the anisotropic refinement details for $K_4Ge_{4-x}P_xSe_{12}$ with positional disorder of Se(3). The refinement results with no positional disorder of Se(3) were obtained by setting its anisotropic thermal parameter equal to that of Se(2) using the EADP command in SHELXTL. The results for the distorted subcell within the modulated refinement can be found in Table 3.
(60) Chondroudis, K.; Kanatzidis, M. G. *Chem. Commun.* **1996**, 1371.
(61) Martin, B. R.; Dorhout, P. K. *Inorg. Chem.* **2004**, *43*, 385.